

The Sissano, Papua New Guinea tsunami of July 1998– offshore evidence on the source mechanism (Marine Geology 2001 175: 1-23)

D. R. Tappin¹, P. Watts², G. M. McMurtry³, Y. Lafoy⁴, T. Matsumoto⁵

¹Corresponding Author
British Geological Survey
Kingsley Dunham Centre
Keyworth, Nottingham,
NG12 5GG
United Kingdom
d.tappin@bgs.ac.uk
Fax: 44 115 9363200

²Applied Fluids
Engineering, Inc.
Mail Box #237
5710 E 7th Street
Long Beach
CA 90803
United States of America
phil.watts@appliedfluids.com
om
Fax: 562 498 9407

³School of Ocean and Earth
Science and Technology
University of Hawaii
1000 Pope Road
Honolulu, Hawaii 96822
United States of America
garym@soest.hawaii.edu
Fax: 808 956 9225

⁴Services des Mines et de
l'Energie
PB 465, 98845
Noumea
New Caledonia
lafoy@noumea.orstom.nc
Fax: 687 27 2345

⁵Japan Marine Science and
Technology Centre
2-15 Natsushima-cho
Yokosuka, Kanagawa
237-0061, Japan
matsumotot@jamstec.go.jp
Fax: 81 468 66 5541

Abstract

The source of the local tsunami of 17th July 1998 that struck the north shore of Papua New Guinea remains controversial, and has been postulated as due either to seabed dislocation (fault) or sediment slump. Alternative source mechanisms of the tsunami were addressed by offshore investigation using multibeam bathymetry, sub-bottom profiling, sediment sampling and observation from the JAMSTEC Dolphin 3K Remotely Operated Vehicle and Shinkai 2000 Manned Submersible. The area offshore of Sissano is a complex active convergent margin with subduction taking place along the New Guinea Trench. Dominant transpressional convergence results in diachronous collision of the highstanding North Bismarck Sea Plate in a westerly direction. The result is a morphological variation along the Inner Trench Slope, with the boundary between eastern and western segments located offshore Sissano in an area of on- and offshore subsidence. This subsidence, together with nearshore bathymetric focusing, is considered to increase the tsunamigenic potential of the Sissano area. The offshore data allow discrimination between tsunami generating mechanisms with the most probable source mechanism of the local tsunami as a sediment slump located offshore of Sissano Lagoon. The approximately 5-10 km³ slump is located in an arcuate, amphitheatre-shaped structure in cohesive sediments that failed through rotational faulting. In the area of the amphitheatre there is evidence of recent seabed movement in the form of fissures, brecciated angular sediment blocks, vertical slopes, talus deposits and active fluid expulsion that maintains a chemosynthetic vent fauna. Dating of the slump event may be approximated

by the age of the chemosynthetic faunas as well as by a seismic signal from the failing sediment mass. Faults in the area offshore Sissano are mainly dip-slip to the north with recent movement only along planes of limited lateral extent. A possible thrust fault is of limited extent and with minimal (cm) reverse movement. Further numerical modeling of the tsunami also supports the slump as source over fault displacements.

Key Words: Tsunami, Papua New Guinea, slumping, seismology, subduction

1. Introduction

The Sissano or Aitape tsunami that struck the north coast of Papua New Guinea (PNG) in the evening of July 17th 1998 left more than 2,000 people dead and 12,000 homeless as three villages were completely destroyed and four more badly damaged (Figure 1) (Davies, 1988a; Kawata et al., 1999). The scale of the devastation resulted in a comprehensive investigation into the cause of the tsunami event that now includes survivors' accounts, onland study, offshore seabed imaging, geological interpretation, seismological analyses, and computer simulations (Davies, 1998a; Kawata et al., 1999; Tappin et al., 1999; McSaveny, 2000; Synolakis et al., submitted). However, the source of the tsunami has remained controversial.

The tsunami arrived at the coast 20 minutes after a Magnitude 7.1 earthquake shook the area and at about the same time (or a little later depending on location) as two major aftershocks (Davies, 1998a; Kawata et al., 1999; Tappin et al., 1999). A maximum wave height of 15 m was recorded. Onshore investigations into the tsunami wave height distribution along the coast, together with the relative timing between the earthquake and the tsunami arrival indicate the local tsunami source to be just offshore and not a direct result of the main earthquake rupture (Davies, 1998a; Kawata et al., 1999). This conclusion is supported by analysis of the frequency spectrum of the earthquake (Newman and Okal 1998; Synolakis et al., submitted). For the local tsunami generated, simulations based on a thrust fault source have met with little success. With a steeply dipping reverse fault neither tsunami magnitude nor the wave-height distribution measured along the PNG coast have been reproduced (Titov and Gonzalez, 1998; Newman and Okal, 1998; Geist, 1998; Takahashi and Kawata, 1998). A horizontal thrust fault mechanism produced a maximum wave run-up of one to two metres (Matsuyama et al., 2000; Synolakis et al., submitted). A slump source was thus proposed as an alternative source mechanism for the tsunami, an interpretation supported by the preliminary interpretation of the offshore data (Tappin et al., 1999). However, a number of authors have continued to model the locally generated tsunami as sourced from a thrust fault (Kikuchi et al., 1999; Matsuyama et al., 1999; Satake and Tanioka, 1999; Tanioka, 1999). There is no doubt that either of the two earthquake rupture mechanisms may explain the far-field tsunami waves observed in Japan (Satake and Tanioka, 1999; Tanioka, 1999).

Here we present a more considered examination of the offshore data in the context of the published onshore and seismological evidence. We offer an interpretation of the active tectonic processes in the region of the tsunami as a context to our assessment of the most likely local tsunami generation mechanism; we also present a new tsunami numerical simulation that supports our conclusions.

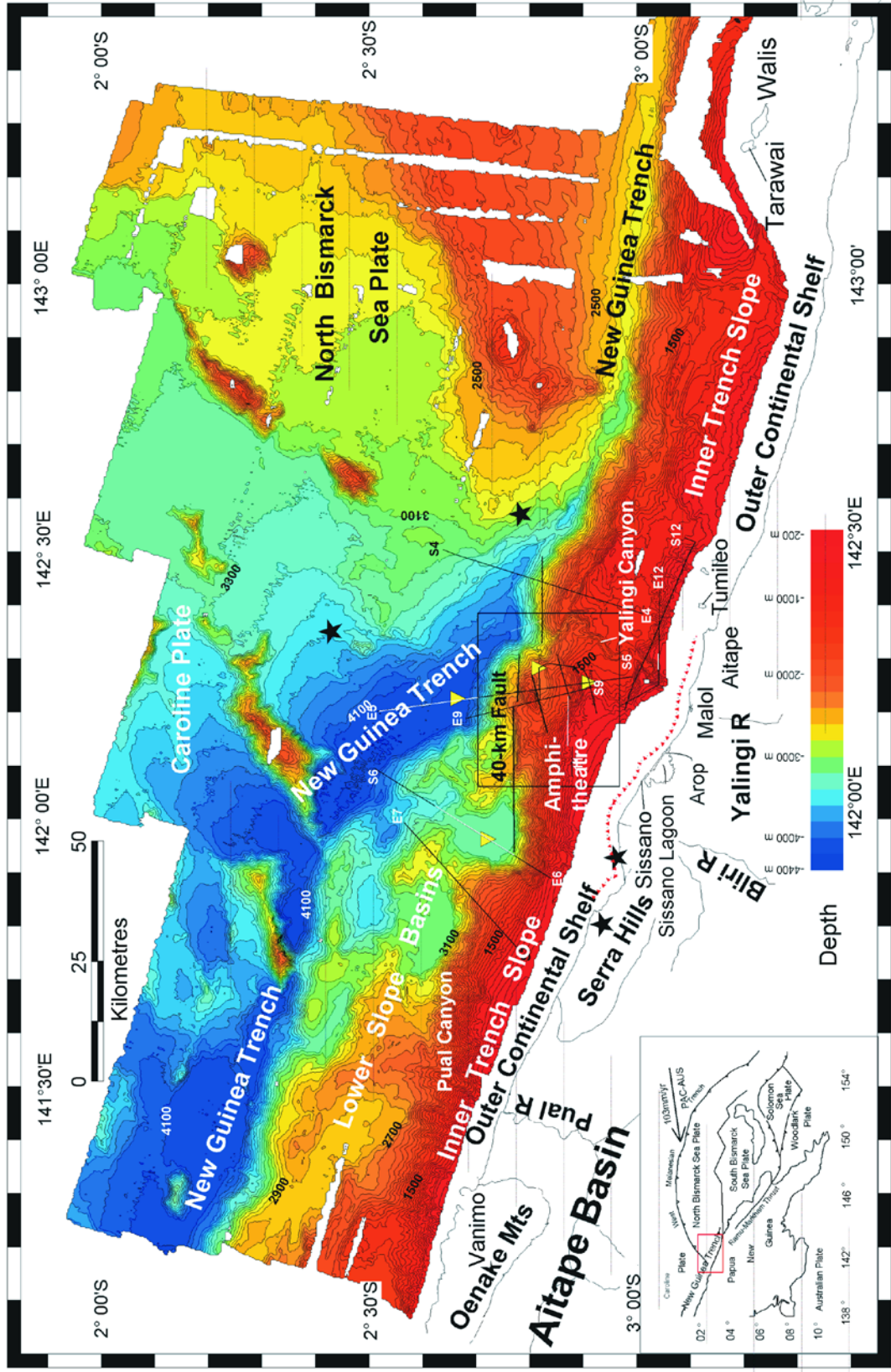


Figure 1. Bathymetry and main morphologic elements offshore of northern Papua New Guinea together with the main coastal locations and features (Box is the area of map in Figure 2). Red triangles = main area devastated by the 17th July 1998 tsunami. Solid black lines = Sub-bottom profiles – white sections are those illustrated in Figure 4 (E=End line, S=Start line). Black stars are alternative epicentral locations for the 17th July 1998 earthquake, although it is recognised that the most likely location is nearshore in the east; Yellow triangles are Core locations. Inset map: Location of mapped area with main plate tectonic elements and plate motions (Red box indicates area of offshore survey).

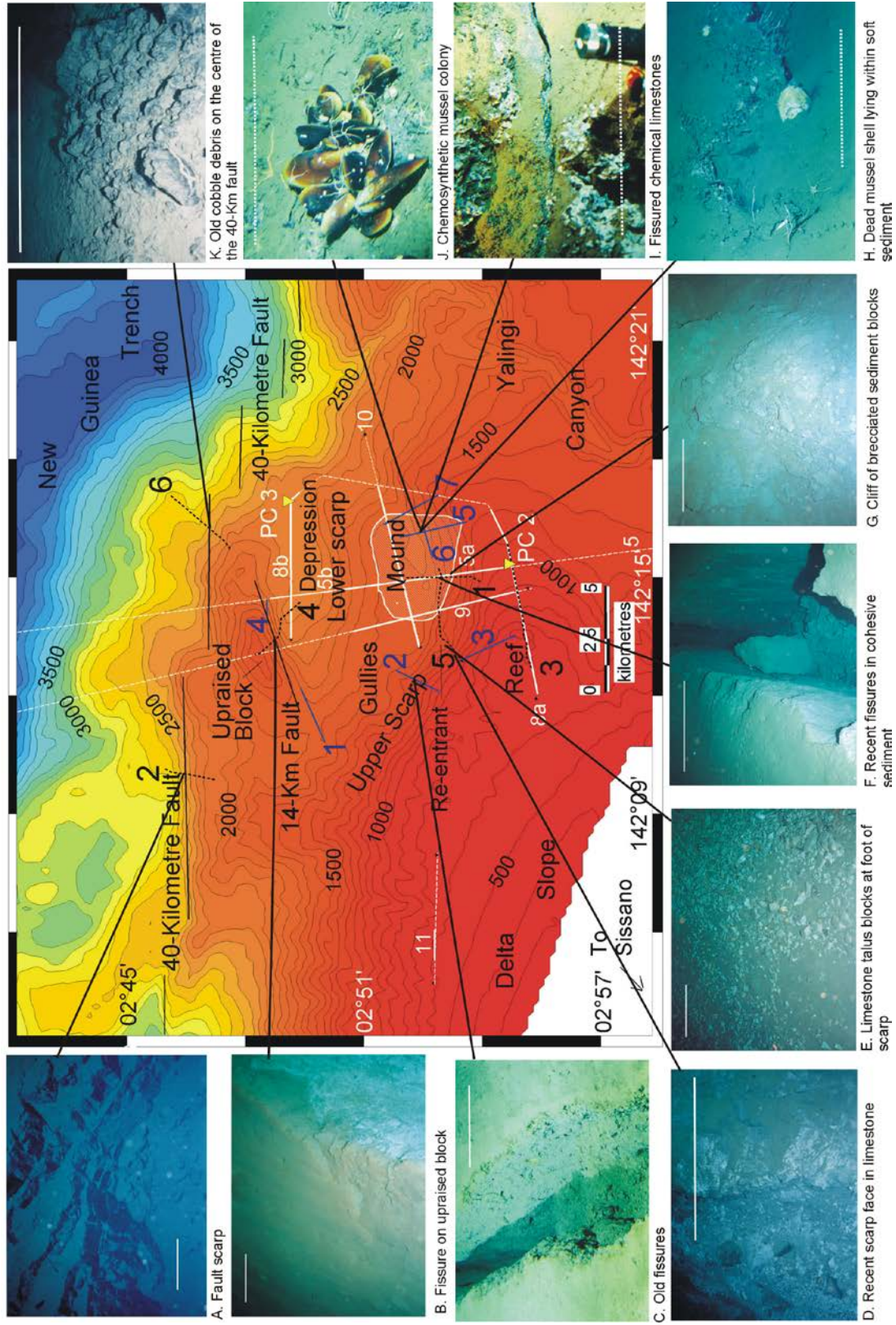


Figure 2. Amphitheatre area off of Sissano lagoon (for location see Figure 1) with main morphologic features labelled and photographs of significant seabed features (Scales: solid white line = 1 metre, dotted white line = 0.5 metre). Solid black lines = Faults; Dashed white lines = Sub-bottom profiles - solid lines those shown in Figure 4; Dashed black lines = ROV traverses; Solid blue lines = Manned Submersible dive traverses; Yellow triangles = Core locations. White hachured area defines the probable main slump area of 17th July 1998.

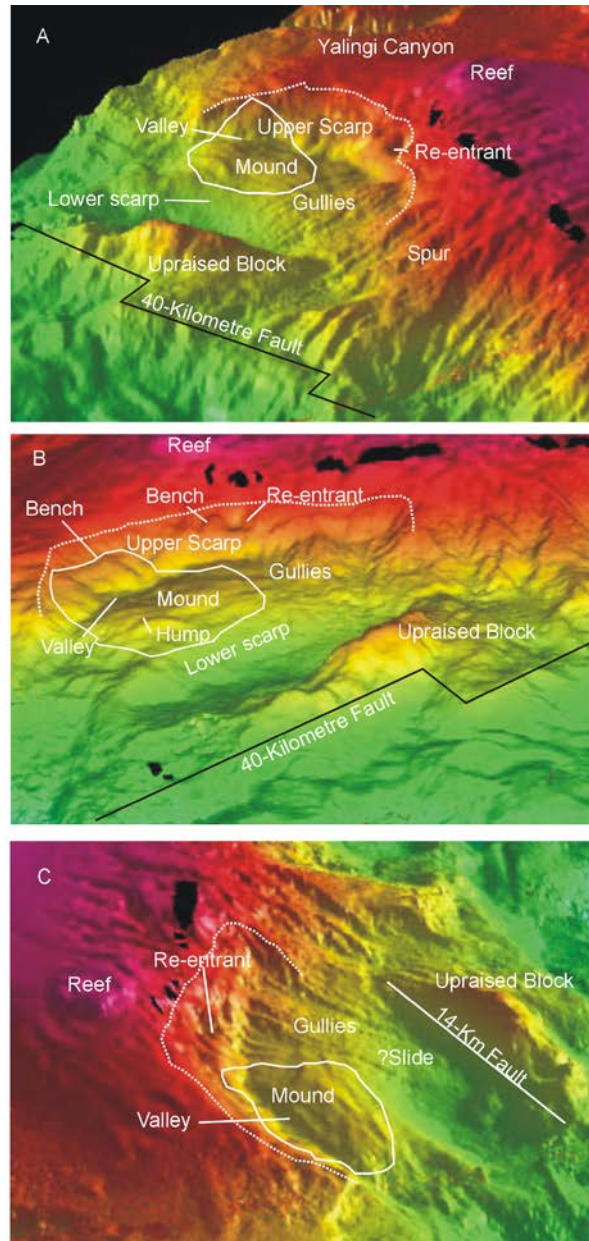


Figure 3. 3-D images of the amphitheatre area: a. from the northwest, b. from the northeast and c. from the southeast. Dotted white line is the top of amphitheatre upper scarp slope; solid white line is the approximate area of the main slump area of July 17th 1998; black areas are data gaps.

2. Regional Geological Setting

Northern Papua New Guinea lies at the boundary between the Australian and Pacific plates that are converging along an azimuth of $\sim 070^\circ$ at ~ 100 mm/year (Figure 1 inset) (Davies, 1990; DeMets et al., 1994; Stevens et al., 1998; Tregoning et al., 1998). The boundary varies

and is complex. In the west it lies along the New Guinea Trench and the Pacific Plate (Caroline segment) is subducted southward beneath PNG. In the east there is a complex of microplates, and convergence is partitioned on the north coast between the North Bismarck Sea Lineation, a sinistral east-west trending transform, and the northward dipping Ramu Markham Thrust. Convergence across the latter decreases westward (Tregoning et al., 1998). The area offshore Sissano Lagoon lies on the western margin of the intersection of these structures (the New Guinea Trench, the North Bismarck Sea Lineation and the Ramu Markham Thrust) as well as the inactive(?) West Melanesian Trench. The New Guinea Trench continues westward where beyond 140°E there is no active convergence and focal plane mechanisms are strike-slip (Seno and Kaplan, 1988; Milsom et al., 1992a, 1992b).

Onshore, the northern part of PNG comprises the E-W trending Aitape Basin that is bounded on the north by the coastal Oenake Mountains and Serra Hills and on the south by Bewani-Toricelli Mountains (Figure 1). The Pual, Bliri and Yalingi rivers drain the Basin northward to the sea. On the eastern margin of the Basin the area is low-lying and the Bliri and Yalingi rivers terminate in deltas with coastal swamps. Here is located the Sissano Lagoon. The dissected morphology of the coastal plain suggests slight uplift after coastal plain formation (Norvik and Huchison, 1980). There is uplifted Quaternary reef limestone on the coast below the Oenake Mountains and that forms the small islands off Aitape (e.g. Tumileo, Figure 1) and the Walis and Tarawai islands in the east. Very young coral reefs around Vanimo and the Serra Hills are over 100 m above sea level. In contrast, the Sissano Lagoon has formed by subsidence, initially during the earthquake of 1907 (Neuhauss, 1911; Welsch, 1998) but with subsidence continuing to the present day (Goldsmith et. al., 1999).

3. The Offshore Surveys – Objectives and Methodology

In early 1999 the Japan Marine Science and Technology Center (JAMSTEC) and the South Pacific Applied Geoscience Commission (SOPAC) carried out two offshore surveys with a third following in September 1999 (Figures 1, 2 and 3). Objectives were to investigate tsunami source(s) (such as faults and sediment slumps) and focusing mechanisms, and to compute a realistic model of the tsunami event. Mapping the offshore regional physiography was also expected to identify the tsunamigenic potential of the area.

Because of safety requirements, the ships surveyed only in water depths greater than 200 m. The first survey, aboard the research vessel *Kairei*, acquired a comprehensive geophysical and sedimentological data set offshore of the north PNG coast between 2° 00'S and 3° 20'S and 141° 00'E and 143° 20'E. Over 19,000 km² of seabed were surveyed using a SEABEAM 2112 multibeam system that produced real-time bathymetry and side-scan sonar image maps. Additionally, 4.2 kHz (high-resolution) sub-bottom profile (SBP) data, piston cores of sediments and gravity and magnetic data were acquired. From the first survey a more restricted area, offshore the Sissano Lagoon, was identified for visual inspection (Figure 2). Here two further surveys aboard the JAMSTEC vessel *Natsushima* acquired observational data (VCR and still photographs) of the seabed together with short (30 cm) sediment push cores and rock and biological samples. On the first survey the tethered, Remotely Operated

Vehicle (ROV) Dolphin 3K was deployed. The second survey utilised the manned Shinkai 2000 submersible.

4. Offshore Surveys - Results

4.1. Multibeam Bathymetry

The bathymetric survey mapped in detail the physiography of the New Guinea Trench and the Pacific Plate comprising the Caroline Plate in the west and the North Bismarck Sea Plate in the east (Figure 1). The Trench is subdivided into an Inner Trench Slope and Trench Bottom. The Continental Shelf itself was not mapped but salient features are described by inference. The dominant structural trend is ESE to WNW and there are along strike variations.

4.1.1. Continental Shelf

The shelf narrows from 10 km in the east to 5 km in the west and is widest between the eastern margin of the Serra Hills and the Tumileo Islands, where it is incised by a major submarine canyon, informally termed the Yalingi Canyon.

4.1.2. Inner Trench Slope

Located between the continental shelf and the New Guinea Trench, there are two major physiographic areas, with the boundary (a transition zone) offshore of the Sissano Lagoon at ~142° 06'E.

4.1.2.1. Eastern Inner Trench Slope

The Slope in the east is 25-30 km wide (Figure 1) with three subdivisions. Farthest east structural trends are E-W; on the lower slope are several linear, normal faults with downthrow to the north; and the upper slope culminates in a bathymetric high around the islands of Walis and Tarawai. At 143° 00'E the structural trend becomes ESE-WNW and the bathymetric high terminates at a mid-slope terrace that narrows to the west. At 143° 42'E a deeply incised canyon on the upper slope is diverted westward above the terrace before terminating at an ESE-WNW trending linear fault. At 142° 30'E the structural trend becomes SE-NW, the upper slope gradient increases and incised canyons extend onto the continental shelf. The mid-slope terrace becomes wider and is sharply divided from a very steep lower slope by a northward throwing normal fault. On the eastern margin of the subdivision is the Yalingi Canyon that meanders and is deeply incised, at several points turning back (to landward) on itself. The Canyon continues onto the shelf to the mouth of the Yalingi River (Figures 1 and 2). At the foot of the midslope terrace it is diverted westward before terminating at a NW-SE trending fault. At the Canyon foot there is no evidence of a submarine fan.

4.1.2.2. Transition Zone

Offshore of the Sissano Lagoon and Bliri River uniform, gently sloping and convex-outward seabed morphology is interpreted as an extension of this low-lying deltaic area (Figures 2 and 3). Numerous channels dissect the northern margin of the uniform seabed area and on the northeast margin, at 500m depth, a circular bathymetric feature 3km in diameter, with an

upraised rim has the morphology of a reef (Figures 2 and 3).

Below the delta, at approximately 700 m depth, seabed gradients increase rapidly and below the reef at between 800 and 2,200 m water depth an arcuate shaped feature is termed here the amphitheatre. In the south, there is an upper, arcuate scarp slope (Upper Scarp on Figures 2 and 3) with very steep gradients that average 45-50°. The steep slope is irregular interrupted by a number of benches of shallower gradient (Figure 3B). Below the reef the scarp curves to the northeast, in which direction its upper depth limit increases to 1,600 m. Westward, the scarp becomes ESE-WNW trending and there is a small re-entrant at 1,300 m. The Upper Scarp terminates at a deeply incised (gullied) spur. At 1,600 m seabed gradients decrease and in the west there is a wide, irregular gently northward-dipping slope that in the east becomes an elongate irregular mound. Below the gently dipping slope/mound, gradients again increase and a less pronounced lower scarp slope descends into an ENE-WSW trending depression with an irregular floor. The western area of the amphitheatre (west of the re-entrant and reef) is deeply incised by canyons and gullies, some of which may be traced into the Depression (Figure 3A and C). The mound expresses greater relief to the east. It is dissected by east-west trending and bifurcating ridges and furrows that in the extreme west are dissected by gullies. The morphology of the amphitheatre suggests formation by sediment slumping.

The northern margin of the amphitheatre is an ENE-WSW trending high, termed the 'Upraised Block' that crests at 1,400 m water depth. Very steep southern and northern margins are interpreted as faults. The ENE-WSW trending southern boundary fault (the 14-Kilometre Fault) downthrows to the south. The linear E-W trending boundary fault in the north (termed because of its length the 40-Kilometre Fault) extends both eastward to the New Guinea Trench and westward to the inner trench slope, terminating at the landward slope of the most easterly of the lower slope basins. It is dissected and offset by a number of north-south trending faults and steepest gradients are in the west. The morphology indicates normal displacement towards the north. Below the 40-Kilometre Fault, to the west and with increasing depth, there are several more arcuate features oriented approximately WNW to ESE.

4.1.2.3. Western Inner Trench Slope

The Slope in the west is over 50 km wide. Upper slope gradients are steeper than in the east and there is a local east-west as well as a north-south depth transition reflected in two series of lower slope basins. A very pronounced upper series decreases in depth from 3,000 m in the east to 2,500 m in the west. Basin floors dip gently landward and terminate against steep and arcuate slopes that are deeply incised by canyons. A large canyon at 141° 30'E (informally termed here the Pual Canyon) extends onto the continental shelf and continues to the mouth of the Pual River. On the uppermost part of the slope, where it trends east-west, there are numerous small incised canyons. The lower series of basins are at 3,500 m and juxtaposed against the New Guinea Trench. They are linear in form. Both sets of basins have lower silled margins.

4.1.3. The New Guinea Trench

The Trench dissects the area (Figure 1) and exhibits along strike variations in morphology. In

the east it is oriented ESE to WNW, is shallowest at 3,000 m and is V-shaped. West of 142° 40'E the trend changes to SE-NW, water depths increase to 4,000 m and the trench is wider with a planar floor. At 142° 00'E the trend returns to ESE to WNW and the planar, flat trench floor remains at 4,000 m. At 142° 00'E and 142° 40'E the trench is intersected by seamount chains located on the downgoing plate.

4.1.4. The Pacific Plate

The boundary between the North Bismarck Sea and Caroline plates is identified by an increase in water depth towards the Caroline Plate that lies between an arcuate line of seamounts between 2° 30'S; 142° 40'E and 2° 10'S; 143° 00'E and the NE to SW trending seamounts to the west. There is no marked trench-like morphology, but following the boundary south and southeastward it merges with the New Guinea Trench. The North Bismarck Sea Plate is characterised by shallow water that in the south rises to an ENE-WSW trending ridge-like feature that crests at 1,400 m. The plate appears to 'intrude' into the Caroline Plate.

4.2. Sub-Bottom Profiles and Sediment Cores

Sub-Bottom Profile's (SBPs) were acquired in the area of the amphitheatre and the Yalingi Canyon (Figures 1, 2 and 4). Four sediment piston cores (KR99-PC-1 to 4) were also acquired (Figures 1, 2, 4 and 5). On the Inner Trench Slope the sediment wedge is seaward sloping with a convex sectional profile that is deeply incised by canyons. NNW of Aitape (Figure 4a, A) and at either side of the Yalingi Canyon, the SBP reveals at least 60 m of well stratified, faulted sedimentary section with internal unconformities. Canyons truncate internal seismic stratification.

On the Sissano Delta front, SBP penetration is 20 m, suggesting that the section is either thin or that the seabed is particularly hard (Figure 4a, B). The reef on the northeast margin of the delta front has an irregular profile and is between 50-100 m high (Figure 4a, C). The reef front is steep and falls away rapidly into the Yalingi Canyon.

The steep slopes of the Inner Trench Slope result in limited SBP penetration and data quality is poor (Figure 4b, A and B). The Upper Scarp of the amphitheatre is irregular and interrupted by benches of shallow gradient. Where gradients are less steep, penetration increases and an acoustically transparent unit underlies the seabed. The unit is traced to the mid-slope bench or mound, where it is 7.5 m thick (Figure 4b, A and B) and onto the upraised block (Figure 4b, E). On the mound the sediments are faulted and in places southward dipping. At the foot of the reef the transparent unit was sampled in core PC-2 (Figure 4a, C and Figure 5) where 8.27 m of homogeneous, cohesive clays were recovered. Sediment shear strength increases from 10 kiloPascals (kPa) at the surface to 30 kPa at 5-6 m depth, below which depth shear strength values fall off rapidly. The sediment at 5-6 m is thus almost over-consolidated. The boundary between high and low values correlates with the lower boundary of the transparent unit seen on the SBPs. Traced farther southeast from the core location into the Yalingi Canyon, unit thickness increases to 15 m and internal reflections appear.

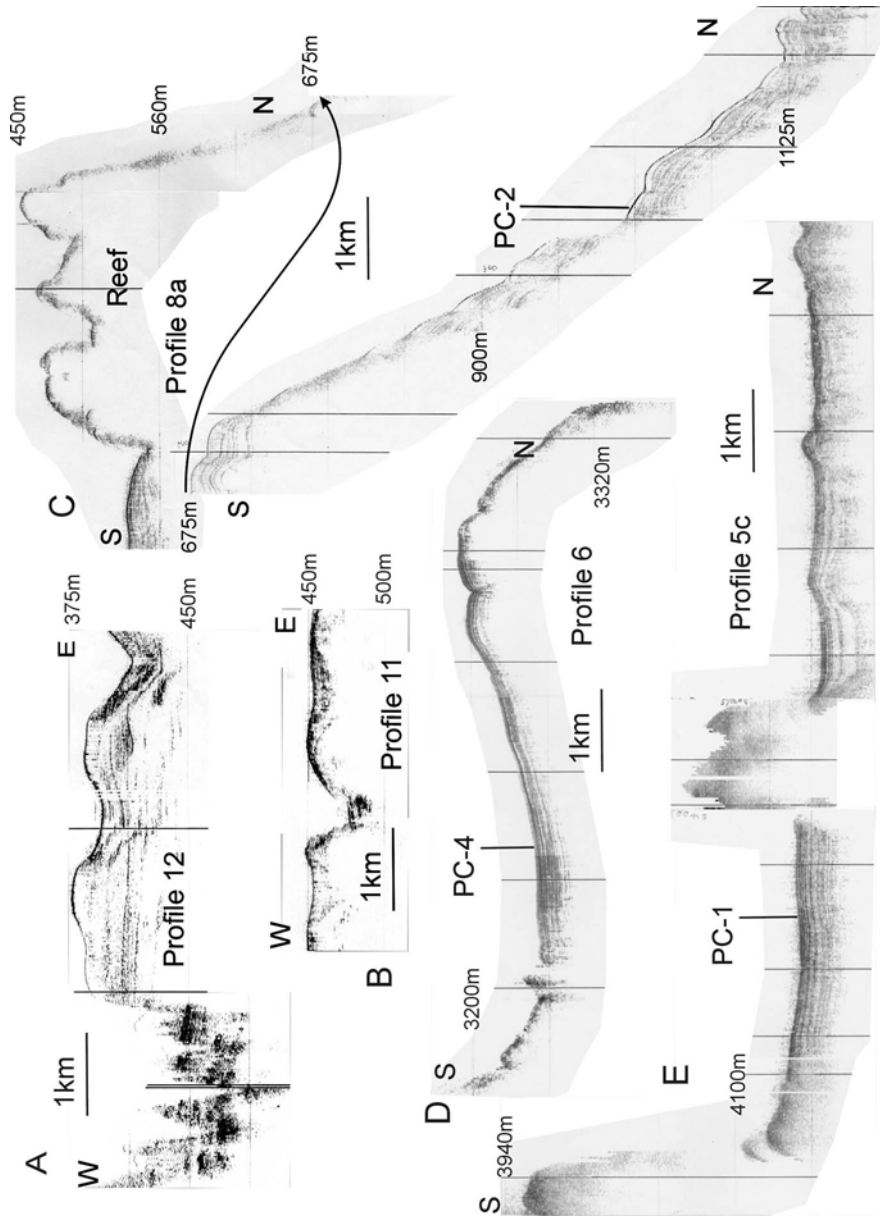
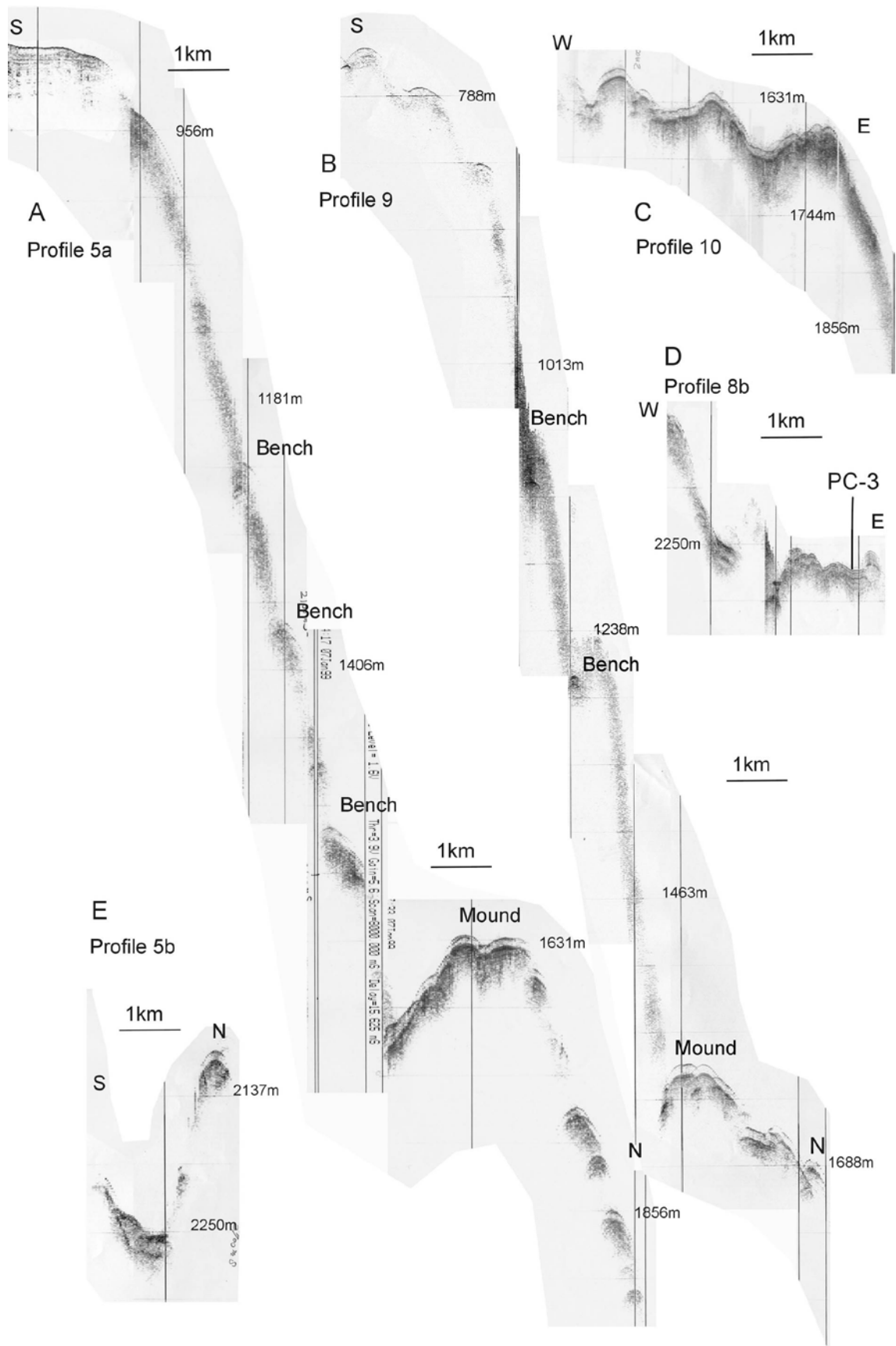


Figure 4. a and b - Sub-Bottom Profiles and piston core locations (with profiles and cores located on Figures 1 and 2). Faint horizontal lines are time lines at 75msec intervals; Vertical lines are time lines. 4a - Profiles located across the Inner Trench Slope (A, B, C), Lower Slope Basin (D) and New Guinea Trench (E); 4b - Profiles located within the amphitheatre area.



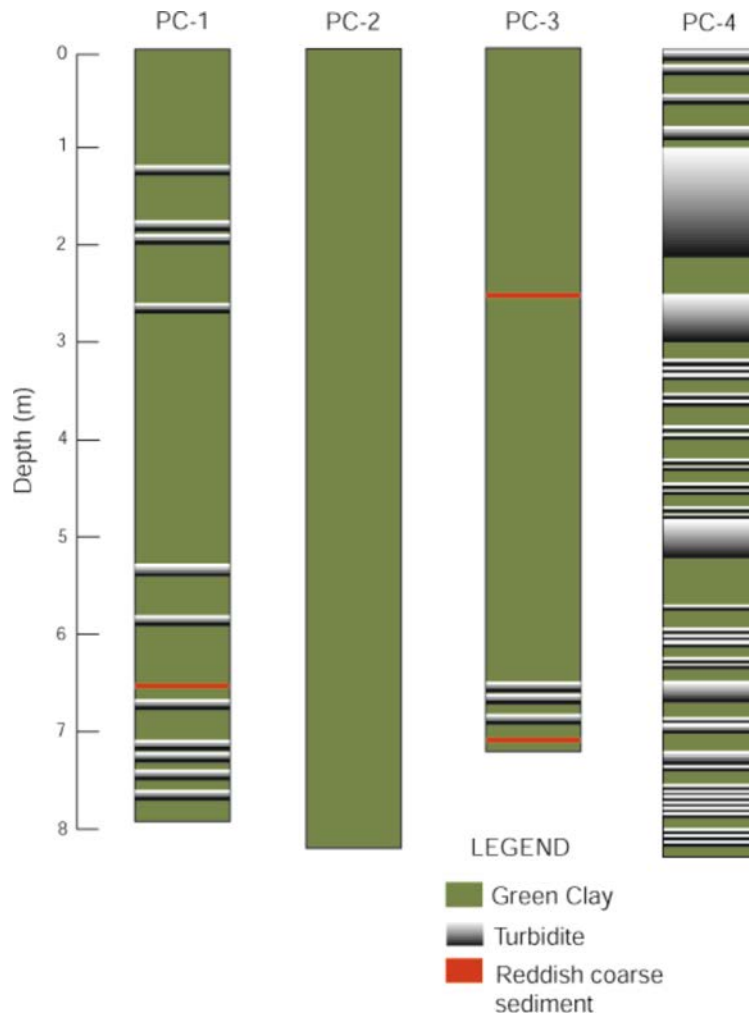


Figure 5. General lithology of piston cores KR99-PC1 to PC4 based upon visual analysis.

The seabed in the Depression at the foot of the amphitheatre has an along strike (east-west) irregular and hummocky profile (Figure 4b, D). Underlying the seabed there is a 25 m sequence of well stratified, faulted and folded sediments, with seabed-parallel stratification. The sediments were sampled in core PC-3 (Figure 5), where 7.19 m of soft mud was recovered with rare bands of coarser silt. On Profile 5b (Figure 4b, E) scarp sediments are seen to be slumping down onto the sediments in the Depression.

To the west of the amphitheatre, Profile 6 (Figure 4a, D) crosses the Inner Trench Slope and the most easterly lower slope basin. On the landward slopes, the gradients are too steep for imaging the sub-seabed, and the profile is similar to that across the Upper Scarp of the amphitheatre. Beneath the inner-slope basin floor there are at least 30 m of undisturbed seismically stratified sediment. Both seabed and sediment layers dip southward towards the landward wall of the basin against which the internal seismic reflections terminate. Sediment

thickness increases in the same direction. At the northern margin of the basin the sediments overlap a sill present there. Core PC-4 (Figure 5) located on the basin floor, confirms the sediments in the basin to be interbedded turbidites and clays.

The floor of the New Guinea Trench (Figure 4a, E) is gently undulating and underlain by a finely seismically layered sequence at least 40 m thick with undisturbed reflections parallel to the seabed. Core PC-1 (Figure 5) was located here and sampled 8 m of soft, well-stratified interbedded turbidites and hemi-pelagic clays.

4.3. Visual Seafloor Images

Six ROV and seven, manned submersible (MS) transects between 500 m and 7 km long were carried out in the area of the amphitheatre (Figure 2). Of these transects, seven traversed the amphitheatre upper scarp and three the southern margin of the upraised block. There was one transect across the reef and two across the 40-Kilometre Fault: one in the east and one in west.

4.3.1. Amphitheatre Upper Scarp

MS Dive 2 was located in the west and followed the eastern side of a spur. Cohesive sediment blocks, dm-sized, subangular and olive-green, lie on the seabed at 1,300 m. Well-bedded, olive-green, cohesive sediment (sampled in a push core) dip steeply. Numerous fissures, striking at 120° at 1,190 m are anastomosing and with rounded margins (Figure 2C). They are 10's m long, ~50 cm deep and up to one metre wide. On the seabed surface there is a dm thick yellow (oxidised) layer. All cohesive sediment surfaces are degraded.

Two ROV surveys traverse the central area. On ROV 1 the seabed on the bench below the scarp foot is featureless except for a single E-W fissure at 1,688 m. Between 1,250 and 1,550 m (with a marked concentration observed below 1,400 m) there are prominent east-west trending fissures located on benches of shallower gradient (Figure 4b, A and B). The fissures are in cohesive clay. Their margins are sharp and vertical with little evidence of margin collapse infill. They are over 50 m long, one metre wide and over three metres deep (Figure 2F). Across the fissures vertical displacement is minimal (cm) and there is a thin (~5 cm) veneer of yellow-brown, soft sediment on the seabed that overlies olive green, cohesive clay. An almost vertical cliff, 10-15 m high at 1,500 m comprises brecciated cohesive sediment (Figure 2G). At the base there are clast-supported angular sediment blocks with little matrix infill and mainly voids between the clasts. Blocks are predominantly equidimensional and estimated at 10-30 cm.

ROV 5 landed at 1,600 m to the east of ROV Dive 1 and traversed a bench at 1,500 metres before ascending into the small, gently northward-sloping, planar-floored re-entrant at 1,360-1,380 metres depth. Numerous sharp sided fissures were traced westward along the 1,500 metre contour with fissure morphology similar to that observed along ROV Dive 1. White bacterial mats were observed and associated with rare tubeworms. A push core driven through a mat recovered dark brown sediment with a strong sulphurous odour. Fissures are present on the floor of the re-entrant, and are small: 10's metres long, 0.5 metres deep and

<1.0 metre wide. Some fissure edges are not sharp, but draped with soft sediment. The southern face of the re-entrant is bedrock, very steep, in places almost vertical that sampling proved to be white limestone on which there is little or no sediment cover (Figure 2D). Below the vertical cliff, the floor of the re-entrant is covered with loose cobble to boulder sized, very angular blocks of limestone that has little or no sediment cover (Figure 2E).

The topmost part of the scarp above ROV Dive 2 was traversed during MS Dive 3. At 900 m depth, a fissure in the cohesive sediment had rounded, eroded margins. Sampling of bedrock at 650 metres, just above the sediment/rock contact proved weathered, recrystallised, cream-coloured coral limestone. Rounded limestone cobbles lie on the seabed.

On three manned submersible dives (5, 6 and 7) on the eastern margin of the Upper Scarp a variety of seabed features were observed. On the mound at the foot of the scarp the seabed is undulating, with fissures in the cohesive sediment as observed previously. On MS Dive 5 the trend of the fissures was 090° and the seabed was lower on the southern side. Fissures were 10's of metres long, up to one metre wide and 0.5 m deep. To the east, on MS Dive 7, there were numerous fissures on the mound trending 045°. Fissure margins were rounded with a sediment drape.

Below the foot of the scarp, dm-sized angular blocks of cohesive sediment lie on the seabed. The lower scarp between 1,677 m and 1,621 m is steep (50°) and intensely, almost chaotically, disturbed. It looks more volcanic than sedimentary. In the cohesive sediment there are fissures (striking ~090°) and arcuate slumps, on the surface of which lie slipped angular cohesive sediment blocks. Fissures anastomose and are 100's m long, metres wide and metres deep. Their sides are vertical and sediment is not eroded. Vuggy limestone lies within the cohesive sediment (Figure 2I) and comprises decimetre thick tabular subhorizontal blocks. Blocks may be *in situ*, but most are slipped as evidenced by their angle of repose and exposed (brilliant white) broken surfaces (Figure 2I). Sediment is predominantly olive-green but the seabed surface is commonly black with sulphides (sampled in a push core) that are associated with white bacterial mats and tube worms. Numerous extant chemosynthetic communities comprise medium brown coloured mussels (*bathiomodiolus* sp.), *Calyptogena* sp, tubeworms and starfish (Figure 2J). Sampled mussel shells are up to 7 cm, *Calyptogena* sp up to 20 cm and tubeworms up to 45 cm. Both mussel and *Calyptogena* sp may be dislodged and lie on and within the sediment (Figure 2H). At 1,621 m the slope gradient decreases to ~40° and the seabed becomes undisturbed. The disturbed seabed area was surveyed by MS Dive 6 between 1,630 and 1,650 m depth and traced along strike for 850 m. Shimmering in the water column indicates active fluid expulsion. Above 1,600 m the gradient averages approximately 20° and the seabed is featureless apart from minor steeper scarps where there is small scale slumping with dislodged cohesive sediment blocks. Above 1,227 m the gradient increases and there are arcuate slumps (60° slopes) on the surface of which lie slipped angular blocks of cohesive sediment. The slumps have brecciated margins and their slipped surfaces are rilled but not weathered. At the top of the amphitheatre scarp between 1,162 and 1,156 m there are a series of en echelon fissures trending 066° that evidence downslope slip.

The most eastern traverse of the Upper Scarp, MS Dive 7 found no evidence of seabed

movement. The seabed was featureless.

4.3.2. Upraised Block

ROV Dive 4 traversed the southern margin of the upraised block (Figure 2) between 2,200 and 1,400 m. The slope at the foot of the block is steep (~20°) and rapidly becomes almost vertical with several rock overhangs. Steepest slopes are between 2,185 and 1,650 m, sediment cover is thin (cm to dm) and there is evidence of between 0.1 and 0.5 m vertical displacement in both rock and sediment. Colour variation within the sediment from yellow-brown (oxidised) at the seabed to olive-green (not oxidised) at depth again suggests recent exposure of the sediment. Vertical fissuring is common with sediment chutes and gullies cut into the bedrock (Figure 2B). At least one fissure with 10-cm vertical displacement was followed for about 100 m along the base of the block. At one location there is an overhang approximately five metres high, but no slickensiding was observed. On shallow slopes the seabed is covered with angular to round cobble to boulder sized blocks that sampling proved to be igneous and metamorphic in origin. There is little sediment cover on the blocks. Above the main areas of fissuring at ~1500 m depth, there were living tubeworms associated with bacterial mats. Sediment cover increased towards the top of the block.

MS Dive 4, to the east of the ROV dive, traversed the steepest part of the southern side of the upraised block. There is near vertical weathered rock at outcrop that is interpreted as an old fault plane dipping south or southeast. No fresh rock faces were observed and all rock observed was very weathered. Chemosynthetic communities of mussels and tubeworms were common and found in association with sulphides and bacterial mats. Living mussels up to 15 cm long were sampled

MS Dive 1 investigated the western side of the amphitheatre to the south west of the Upraised Block. The seabed was featureless until the base of the amphitheatre upper scarp slope was reached, where evidence of sediment slumping was observed.

4.3.3. Submerged Reef

ROV Dive 3 was an ENE-WSW traverse along a spur that extended from the northeast side of the reef identified on the multibeam bathymetry and out towards the Yalinga Canyon (Figure 2). The deeper section of the dive from 1,000 to 700 m crossed a sediment covered slope, at the top of which are blocks of vuggy coral limestone. From the reef base at 700 m an almost vertical cliffed face rises to a crest at 460 m. In hollows on the reef top are accumulations of dead 'fingers' of the branching coral, *Acropora* with no sediment cover. The fingers are degraded but readily identifiable. The top and sides of the reef are fractured and fissured. Samples from the reef are of coral limestone and platy algal limestone interbedded with lithified green mudstone of similar type to that sampled in core PC-2. The algal limestone is similar to that usually found on a reef platform in an intertidal environment. On the reef front disarticulated *Calypptogena* sp(?) shells were observed and on the reef-top, samples from live mussel beds and tubeworm colonies were acquired. The mussels are black in colour and shells up to 17 cm long were sampled. Tubeworms up to 65 cm high were sampled.

4.3.4. 40-Kilometre Fault

The north-south ROV traverse between 2,648 m and 2,052 m (Dive 2) traversed the western segment of the fault (Figure 2). The landing site was sediment covered with cobble sized rounded and angular rock debris at 2,645 m and fresh angular rock debris at 2,539 m. Seabed between 2,600 and 2,550 m has a thick veneer of rounded to angular rock debris. Between 2,500 and 2,400 m it was steep to near vertical and comprised well-bedded sedimentary rock dipping to the north or northwest that sampling proved to be sandstone and mudstone (Figure 2A). Both seabed rock debris and bedded strata were either exposed or covered with a thin sediment veneer. The near-vertical face is interpreted as a fault with downthrow to the north. Above it there was a sediment covered seabed slope of shallow gradient.

The northeast to southwest traverse across the central segment of the 40-Kilometre Fault (ROV Dive 6) was between 2,635 and 2,066 m water depth. In its lower part the slope was steep and sedimented with chutes, small-scale slump structures, and at least one possible fissure in the sediment that was oriented NE-SW. The fissure is 100's of m in length and evidenced a vertical displacement of 10 cm. Some of the ridges strike across the slope. At the top of the traverse at 2,164 m, rock exposed at the seabed was sampled and proved to be very weathered and/or altered (?)basalt (Figure 2K).

5. Interpretations

5.1 *The regional context from offshore data*

The bathymetry confirms the geological complexity of the area (Figure 1). We have mapped the boundary (almost a 'triple' junction) between the Caroline and North Bismarck Sea plates where, along the New Guinea Trench, they converge with the Australian Plate.

In the east, collision with the shallow-water (upstanding) North Bismarck Sea Plate results in a V-shaped trench, that becomes deeper and wider westward, and a narrow, structurally varied, Inner Trench Slope. The base of the Slope is interpreted as undergoing predominantly strike-slip deformation with a dip-slip component resulting in subsidence into the Trench. The change in orientation of the faults, from E-W in the east to SE-NW in the west is attributed to the diachronous westward collision. The collision results in the offset and diversion (as well as the termination) of the lower sections of the submarine canyons (most notably the Yalingi) that dissect the upper part of the inner trench slope. A seismic line located on the eastern margin of the area (Davies, 1990) shows a 1,000 m thick, undeformed sediment section on the North Bismarck Sea Plate juxtaposed against the Inner Trench Slope. There is no accretionary prism developed and the absence of deformation suggests mainly strike slip movement.

Westward of 143° 00'E the presence of the mid-slope terrace (together with its development and progressively landward offset to the west) suggests that normal (trenchward directed) downfaulting increasingly deforms the upper part of the inner slope in a westward direction. The subsidence of the upper slope extends furthest landward in the vicinity of the Yalingi Canyon and extends onshore in the area of Sissano. Back tilting of the upper inner slope is evidenced by the sharp (landward directed) bends along the length of the Yalingi Canyon. However, an alternative mechanism to explain the backtilting in the Yalingi area may be by

northward directed shallow-dipping northward overthrusts. The most probable rupture mechanism of the 17th July 1998 earthquake was a shallow dipping overthrust (Goldsmith et al, 1999; McCue et al., 1998; McSaveny et al., 2000) although this is disputed (Tanioka, 1999; Kikuchi et al., 1999).

By contrast in the west, where water depths over the Caroline Plate are greater (the Trench is over 1,000 m deeper) the morphology indicates a more extensional form of deformation. The wider inner trench slope and the back-tilted lower slope basins that descend the Inner Trench Slope are comparable to those present on fully intraoceanic extensional island arcs such as Tonga (e.g. Herzer and Exon, 1985; Tappin, 1994).

The change in the morphology and style of deformation along the inner trench wall takes place just offshore Sissano (Figure 2) although subsidence extends onshore. The Sissano Lagoon has subsided over the past 100 years (Neuhauss, 1911; Welsch, 1998; Goldsmith et al, 1999). Within this transition zone there is mainly extensional deformation and subsidence of the inner trench slope. Immediately offshore of the Lagoon, the reef on the northeast margin of the delta front has subsided to 500 m from the intertidal zone. Below the reef, the arcuate morphology of the amphitheatre indicates formation by subsidence and slumping. The 40-Kilometre Fault downthrows to the north and the most recent movement (~100 metres throw) is confined to the western segment. Slumping may also have formed the arcuate structures below the 40-Kilometre Fault. There is however secondary transpression that results in the Upraised Block, that is most likely formed by limited local movement between its bounding faults: the 40-Kilometre Fault on the north and the 14-Kilometre Fault on the south. The latter fault is interpreted as a small (cm-dm scale) overthrust to the north that may represent the surface expression of the July 1998 main shock rupture.

Onshore, deformation is mainly strike-slip although there are large vertical displacements (4,000 m; Norvick and Hutchison, 1980). Focal mechanism solutions for recent earthquakes indicate a combination of strike-slip movement and compressional overthrust (Johnson and Molnar, 1972; Ripper, 1975). A shallow dipping, northward directed overthrust has been cited as the cause of the subsidence of the Sissano Lagoon (Goldsmith et al, 1999). To the east, northward thrusting along shallow-dipping structures may account for the presence of the uplifted highs on the inner slope, that culminate in the Walis and Tarawai islands in the east and in the Tumileo islands in the west. To the west the highs are progressively offset landward, finally forming the Serra Hills and Oenake Mountains onshore. Complex deformation is not unique to this area. Farther west a confusion of thrust and strike slip faulting has also been observed in western Papua New Guinea and Indonesia, and is attributed to the complex deformation in the region (McCaffrey and Abers, 1991). To the east convergence between the Pacific and Australia plates is partitioned between the Ramu-Markham Thrust and the New Guinea Thrust Belt (Tregoning et al., 1998).

The difference in morphology and deformation between the east and west is attributed mainly to the different type of oceanic crust being subducted at the New Guinea Trench. In the east the North Bismarck Sea Plate probably originated as a backarc basin on the south side of the West Melanesian Trench, thereby explaining its lower density (and elevated position). The

Caroline Plate, in contrast, is truly oceanic (Hegarty and Weissel, 1988). The difference in crustal density (and thus present elevation) results in subduction in the east being more compressional than in the west. Variation in plate coupling is supported by focal plane mechanism solutions that indicate mainly strike-slip faulting in the east and normal faulting in the west (USGS web page). The deformation identified in the Sissano area is almost certainly attributable to its location at the boundary between the two areas and to the dominantly strike-slip convergence that results in the collision of the North Bismarck Sea Plate at the New Guinea Trench. West of Sissano, the numerous incised canyons on the inner trench slope and basin headwalls, together with sediment overlap on the silled outer margins of the inner slope basins, suggest that the rate of subduction erosion is low. The low level of seismic activity in this area (Seno and Kaplan, 1998) also suggests the rate of subduction may be low or dormant.

5.2 The sedimentary regime

Contrary to what might be expected in a region experiencing onland uplift, in combination with a tropical climate, sedimentation rates on the inner trench wall appear to be limited, although there are variations within the area surveyed. The common presence of deep, mainly linear, canyons and gullies on the steeper slopes indicates active and in part localised erosion. There is no evidence of submarine fan development at the bottom of any submarine canyons. In the area of detailed survey our seabed observations suggest a great variation in sediment thickness. Unlithified sediment is observed closely juxtaposed with lithified basement of both sedimentary and volcanic character.

The sediment in core KR99-PC-2 (Figure 5) and in several sediment cores collected by the ROV/Submersible, together with the limited penetration on the SBPs (Figure 4) suggests that on the steep slopes the sediment is homogeneous, stiff and cohesive clay. In depressions, at the foot of the amphitheatre, in the lower slope basins and on the floor of the trench the greater acoustic penetration on the SBPs together with core samples indicate that sediment is softer and more variable (turbidites). Turbidites are most common in the lower slope basins, less common in the trench and at a minimum in the Depression at the base of the amphitheatre. Greater SBP penetration in the Yalangi Canyon area suggests a greater (and softer) sediment thickness here, although there is also active erosion taking place as evidenced by the truncation of internal reflectors on the SBPs (Figure 4a, A). The presence of unconformities on the SBP records also indicates slight deformation, probably associated with subsidence.

Onshore controls on fluvial sediment input to the offshore area include the size of the catchment area as well as onland topography. The catchment area of the three rivers is limited, bounded as they are in the south by the Bewani-Torricelli Mountains and in the north on the coast by the Oenake Mountains and Serra Hills. The drainage in northern PNG is thus concentrated along the eastward flowing Sepik River to the south of the Bewani-Torricelli Mountains. Fluvial sedimentation is localised along three main rivers, the Pual, Bliri and Yalangi. However, only the Pual and Yalangi discharge fully into the sea (creating the canyons offshore) as the Bliri terminates in the swamps and delta surrounding the Sissano

Lagoon. The greater thickness of sediment in the Yalingi canyon area may also be attributable to subsidence in this area.

5.3 The offshore evidence on the local tsunami source and focusing

Evidence from the onshore surveys indicates that the tsunami originated close (~25 km) offshore of Sissano (Davies, 1998a; Kawata et al., 1999). The wave intensity was focused along a narrow (40 km) band of coast with maximum wave height at the sand spit. Wave incidence was from the east at the Bliri River, directly from the sea at the Lagoon Spit and from the west at Aitape. The location of the earthquake and the timing of the arrival of the wave in relation to the earthquake also indicate a local source. The most likely local tsunami source area is thus considered to be the amphitheatre area (including the 40-Kilometre Fault) offshore of Sissano lagoon. Two alternatives are considered; thrust fault and sediment slump.

5.3.1 Evidence for a fault source

Modeling of the local tsunami from a thrust fault source requires a 40-kilometre long reverse thrust averaging 2 metres of vertical movement (Titov and Gonzalez, 1998; Newman and Okal, 1998; Geist, 1998; Takahashi and Kawata, 1998; Kikuchi et al., 1999; Matsuyama et al., 1999; Satake and Tanioka, 1999; Tanioka, 1999; Geist, 2000; Synolakis et al., submitted). If these models are correct the thrust would necessarily be a steeply dipping overthrust to the south (Synolakis et al., submitted). Relative seabed depression to the south is required because the tsunami was a leading depression N-wave (LDN) event (Tadepalli and Synolakis, 1994; 1996; Kawata et al., 1999).

On the offshore surveys no seabed expression of a thrust fault of appropriate size was located. The 40-Kilometre Fault would fulfill the onshore evidence for the local tsunami source and would generate a tsunami that would concentrate on the Lagoon (Matsuyama et al., 1999). However, it is not southward-directed thrust but has a normal throw to the north and is recently active only along its western segment. Alternatively, the 14-Kilometre Fault throws south but is too short and only evidences minimal overthrust throw (maximum of 0.4 metres) along a limited length (>1 km). Recent deformation along this fault is indicated by the common presence of the chemosynthetic faunas and algal mats with sulphide deposits. Another possible tsunami source is a 'blind thrust', that did not break the seabed surface. In this instance we would still expect evidence of some seabed movement. In convergent margins, where there is a lack of an accretionary prism, such as New Guinea, an earthquake rupture would be expected to reach the surface (Kanamori and Kikuchi, 1993).

5.3.2 Evidence for a slump source

The arcuate morphology of the Upper Scarp of the amphitheatre indicates a formation through sediment slumping, probably during several events of different ages. It is probable that the most recent failure is complex (Figure 3). The Upper Scarp we would describe as the slump headwall. The upper failure plane has at most a ~60-70 m high detachment surface traversed on MS Dive 5. The surface expressions of the detachment are the areas of exposed cohesive sediment (with rilled surfaces) observed on the steeply dipping surfaces at the top of MS Dive

5 and the brecciated cliff at 1500 m on ROV Dive 1. In the east, the benches on the headwall are interpreted as the top of individual slipped cohesive sediment slump masses. The fissures on these shallow dipping benches are formed by extension as the sediment mass failed. The small vertical displacement across the fissures suggests them to be the surface manifestations of deeper-seated failure planes in a thick sediment section. The complex morphology of the benches with prominent examples being located at different elevations on the Upper Scarp (see Figure 3B) indicates that the slump is formed of several component parts.

The mound at the foot of the Upper Scarp we interpret as formed by upthrusting created by the slipped sediment mass. The ridges and furrows, with internal reflections dipping towards the Upper Scarp, formed by this mechanism. The fissures are an expression of the thrusting with the northern fissure margins higher than those on the south, as would be expected. The valley between the Mound and the Upper Scarp (Figure 3) indicates a major fault to be located here.

The east to west variation in morphology we interpret as due to along strike variation in failure mechanism. In the west (the area of gullying) slumping may be traced into the Depression below the Upraised Block (Figure 3A) and suggests a translational mechanism of failure of a disintegrative type and with sediment transported downslope. By contrast, in the centre and east slumping does not extend into the Depression. The failure is more localised and confined between the top of the Upper Scarp and the northern margin of the Mound. Rotational slumping is suggested. Towards the east the increase in the height of the Mound, together with a pronounced 'hump' in this direction (Figure 3), suggests slumping to be concentrated in this eastern area. A corresponding prominent convex outward feature on the headwall above the hump supports this proposition. The southward slope of the Mound into a valley between the Mound and the Upper Scarp indicates the presence of a major fault between these two areas. In the east, the concentration and extent of fissuring, the high level of fluid expulsion features (shimmering, algal mats, chemosynthetic communities and sulphide rich sediment) together with the major sediment disturbance at the foot of the Upper Scarp support the likelihood of a major slump here. The eastern limit of the slump is defined by Submersible dive 7 on which no seabed structure on the Upper Scarp was seen.

From the top of the Upper Scarp to the northern margin of the Mound the proposed length of failure is approximately 5 km. With a typical 15% maximum thickness to length ratio, this 5 km dimension allows us to predict a 750 m thick rotational slump in cohesive sediment (Schwab et al., 1993; Turner and Schuster, 1996). On a multichannel line acquired across the eastern part of the amphitheatre a displaced sediment mass up to 740 metres thick has been interpreted with a cross sectional area of 2.3 km² (Sweet and Silver, in press). We estimate the slump to be approximately 5 km wide. Based on the cross-section and our estimate of the slump surface area, we estimate the slump volume to be between 5-10km³.

The presence of such a large slumped mass in the east may be accounted for by a variation in sediment thickness within the amphitheatre. In the east of the headwall, in the re-entrant, exposure of bedrock indicates thinner sediment here than in the east. We suggest that sediment thickness increases eastward. This thickness variation may account for the failure(s) in the west being translational rather than rotational. It is also considered probable that there is

a control fault at the head of the slump.

Relative timing of failures in the amphitheatre may be identified from our data. In the west, the deeply incised morphology is similar to the landward scarps on the lower slope basins to the west. The numerous seabed fissures, exposed dipping sediments and slump scars with slipped sediment blocks (compare Figures 5A and 5B) are degraded. There is an absence of fluid expulsion, expulsion features and chemosynthetic communities. Chemosynthetic communities have been used by Orange et al. (1999) off California as evidence for different levels of fluid expulsion that have been related to seabed faulting and slumping. Overall these observations indicate that seabed movement in the west is not of recent date.

In the centre and east of the amphitheatre the morphology suggests a different history. The absence of canyons and gullies and the less rugged seabed suggests the deformation here to be more recent than in the west. The preservation of the seabed features also indicates a recent origin, for example the fissures have sharper margins and the slump scars on the headscarp are undegraded with displaced angular 'fresh' sediment blocks. Toward the east there is an increase in the variety and concentration of the chemosynthetic communities. In the west these communities are absent. In the centre of the headscarp there are rare bacterial mats and tubeworms and faunas increase towards the east. There are algal mats, tubeworms, mussels and *Calyptogena* sp. Shells are commonly displaced downslope. There is active fluid venting and the seabed sediment is commonly sulphide rich. Displaced limestones within the seabed sediment have fresh surfaces. The faunas and fluid expulsion are both concentrated at the base of the upper headwall in the valley where it meets the Mound.

5.3.3 *The slump mechanism*

An essential aspect of assessing tsunami risk by slumping is a consideration of the type and volume of sediment present. It is well known that stiff clays are more likely to cause tsunamigenic mass failure than soft sediment and that the mechanism of failure controls the magnitude of the tsunami wave produced (Turner and Schuster, 1996; Watts et al., submitted). Alternative mechanisms of sediment failure range between soft sediment deformation, as in turbidites (disintegrative), to rotational slumps in cohesive sediments (non-disintegrative) (Schwab et al., 1993). Rotational slumps have a greater tsunamigenic potential.

From the evidence acquired, we suggest that in the amphitheatre, failure in the east was by rotational slumping with the decollement at the contact between the cohesive sediment and bedrock. There is no evidence for large-scale turbidity flow, quite the opposite in fact, as the turbidites in all the cores are relatively thin. At the base of the amphitheatre, PC-3 sampled soft clay with several turbidites near the base. On the SBPs, internal reflectors are disrupted indicating deformation *after* emplacement. This would not be anticipated if the turbidity flow took place in 1998. A small slump on the lower scarp progrades *over* the sediments in the Depression. There may in fact be several recent minor slumps along the perimeter of the amphitheatre with scales of hundreds of metres. However, one recent slump stands out as being much larger than the other suspected failure sites, and is consequently much more tsunamigenic.

5.3.4. Evidence of Recent Seabed Movement

There is no doubt that the area off Sissano Lagoon has been subject to recent seabed shaking as shown by the sharp edged fissures, angular talus slope deposits, fractured limestone, brecciated vertical scarps and slumped and brecciated cohesive sediment blocks. These features are almost certainly the result of earthquake shaking and/or sediment slumping. We have suggested that older and younger seabed features are present and that *by comparison* the features in the east appear younger. We cannot date these features directly yet two intriguing lines of evidence may illuminate this temporal dilemma: the chemosynthetic communities and acoustic waves in the SOFAR channel.

5.3.4.1. Significance of the Seeps and Chemosynthetic Communities

The discovery of extant chemosynthetic bacterial mats, mussels, *Calyptogena* sp. and tubeworms in the amphitheatre region indicates the active expulsion of sulphide- and methane-rich pore fluids from the sediment (Paull et al., 1984; Hecker, 1985; Suess et al., 1985; Kulm et al., 1986; Paull and Newman, 1987; Le Pichon et al., 1987). The spatial variation and style of the faunas provides evidence on the mechanisms controlling fluid expulsion, the chemical composition of the fluid, and the levels of fluid flow (Orange et al., 1999). On the landward scarp slope of the amphitheatre there are distinct variations with an increase in fauna eastward. In the west, faunas were not observed; in the centre, there are isolated bacterial mats and rare tubeworms; and in the east there is a profusion of bacterial mats, mussels, *Calyptogena* sp and tubeworms. The bacterial mats are intimately associated with black sulphide-rich sediments lying at the seabed. Additionally, there is active fluid venting. On the 14-Kilometre Fault there are bacterial mats, mussels and tubeworms. On the reef there are mussels and tubeworms. No extant faunas were observed on either traverse of the 40-Kilometre Fault. We conclude that fluid expulsion is most active at the eastern part of the amphitheatre landward scarp with subsidiary activity along the 14-Kilometre Fault.

Observation and sampling of the faunas show that smaller, more juvenile forms are located in the east. Mussels of 15 to 17 cm length were sampled on the subsided reef and 14-Kilometre Fault. In the east they are smaller at 7 cm length. In hydrothermal areas initial growth rates of mussels have been measured at up to 4-6 cm per year, decreasing logarithmically as they age to up to 20-30 years when they approach 20 cm shell length (Turekian and Cochran, 1981; Lutz et al., 1985). Cold seep mussels from the Gulf of Mexico grow slower and reach smaller maximum lengths (Nix et al., 1995; Smith et al., 1997, 2000); however, the seep mussels here reach maximum lengths similar to those of the hydrothermal variety and may therefore grow at similar rates. The 7 cm long mussel shells suggest an age of 1-2 years if growth rates are similar to those at some hydrothermal locations. The submersible survey on which the samples were acquired was carried out 14 months after the tsunami struck. It is therefore probable that the initiation of active venting in the east is very recent and is associated with the observed slumping.

There is a concentration of fluid expulsion at the base of the amphitheatre landward scarp. In Monterey Bay, California, Orange et al. (1999) observed a strong relationship between geomorphology and cold seep fluid flow. Here both active and dormant seeps are restricted to

the scarps of canyon walls and slope failures. Both create bathymetric indentations that focus fluid expulsion if the head gradient is above hydrostatic. For slope failure the alternatives are fluid expulsion as the source or result of rupture (or slumping in this case) (Sibson, 1981a; 1981b). An intriguing aspect of our study is the identification of slipped tabular limestone in the eastern amphitheatre landward scarp. In morphology and association it appears to be authigenic. Authigenic limestone is often a precipitate of pore fluids high in bicarbonate which is derived from the bacterial oxidation of methane or other carbon sources (Roberts and Whelan, 1975; Ritger et al., 1987; Hovland et al., 1987; Botz et al., 1988; Neumann et al., 1988; Kulm and Suess, 1990; Matsumoto, 1990; Jorgensen, 1992; Paull et al., 1992). Its tabular form suggests low and diffuse fluid flow (Kulm and Suess, 1990; Campbell and Bottjer, 1993). Restricted fluid expulsion through the fine clay sediments may have led to hydrofracturing that resulted in slope failure ultimately triggered by the earthquake.

5.3.4.2. Slump sound signature?

Another intriguing piece of evidence on the timing of the slump comes from a peculiar seismic record timed by the United States Geological Survey (USGS) at 09:02 GMT on the 17th July. This record is an aftershock with a body wave magnitude 4.4. Analysis of T-phase radiation through the SOFAR channel indicates this seismic radiation to be caused by a failing slump (Synolakis et al., submitted). The amplitude of the seismic radiation is significantly smaller than other aftershocks of similar body wave magnitude and, to compensate, the record lasted around 65 seconds. This is significantly longer than the 10-second records from other aftershocks of similar magnitude. The frequency content shows a rise and fall in time indicating an accelerating and decelerating source. The epicenter of the seismicity is located at 2.85°S and 142.26°E and corresponds (within 10 km horizontal error bars) to the amphitheatre mapped during the offshore surveys.

5.3.5 The location of the source and temporal relation to the coast

The tsunami arrival time varies with location along the coast: reported to be shortly before the aftershocks at Sissano Lagoon, immediately after at Malol and five minutes later at Aitape (Davies 1998a; Kawata et al., 1999). The most likely earthquake epicentre is on the coast or just offshore to the west of the Sissano Lagoon and the aftershocks to the north of the Lagoon (Figure 1). However, a tsunami sourced from a location to the west of the Lagoon would have arrived at the **nearest** coast (Serai) within minutes (Figure 1) and resulted in the highest runup in the Serai area. Although there are errors in locating earthquake epicentres in this region (Hurakawa, 1998), the earthquake epicentral location is too close inshore (?onshore) and too far to the west to explain, not only the timing and the runup, but also the wave incidence on the coast (Davies, 1998b; Kawata et al. 1999; although see MacSaveny et al. 2000). Similar arguments apply to the aftershocks as a tsunami source. The wave arrived at the coast at the same time as the aftershocks at Malol and five minutes later farther east at Aitape. Travel time to the nearest point of land from the aftershock locations varies from 8-10 minutes.

5.3.6. Local focusing effects

A tsunami sourced offshore of the Sissano Lagoon and propagating southward would refract around the shallow water area off the sand spit. The refraction would be exaggerated by the deep water of the Yalingi Canyon to the east, thereby focussing the tsunami wave onto the

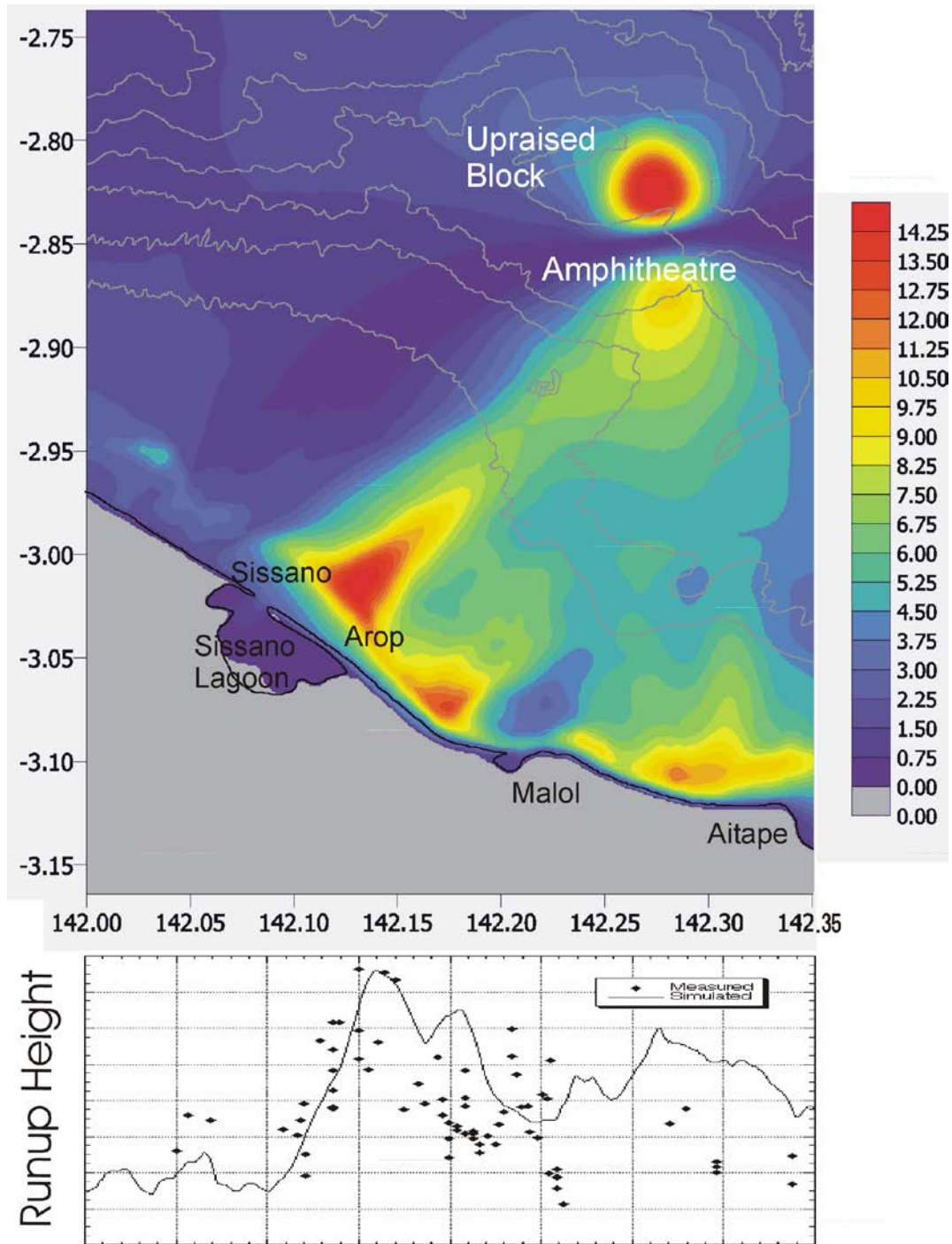


Figure 6. Upper. Time-lapse image of the maximum wave elevation in metres within the simulation domain of a 130 m grid. Wave focusing and shoaling by bathymetric features is clearly evident. Depth contours are in 500 m intervals. Lower. Simulated wave maxima agree quite well with maximum water elevations measured onshore.

sand spit in front of the Lagoon (Matsuyama et al. 1999). However, the factor of two to three increase in tsunami amplitude attributed to focusing is not uncommon in complicated coastal waters and does not suffice to explain the tsunami amplitude. We describe new tsunami simulations below that account for most local facts and observations with a single slump source.

6. New Tsunami Simulations

We have prepared a new simulation based on a slump tsunami source located in the eastern half of the amphitheatre. The simulation technique involved a novel combination of five steps. We first noted that the mode of failure was deep-seated rotation of a cohesive material. Then, we determined the slump shape from both the multibeam data and the seismic profile of Sweet and Silver (in press). Third, we calculated an approximate slump motion that was tailored to the local geology and the observed distance traveled by the center of mass. Fourth, we incorporate the slump shape and motion into a complete fluid dynamic simulation of tsunami generation (Grilli and Watts, 1999). Following tsunami generation, we input the tsunami shape into an accurate tsunami propagation and runup model (Imamura and Goto, 1988). This five-step tsunami simulation technique is further described and justified in Watts et al. (submitted).

The new simulations (Figure 6) demonstrate not only the focusing of the tsunami wave onto the Lagoon but also for the first time approximate both the magnitude of the tsunami wave as well as the wave height distribution along the coast. The work of Synolakis et al. (submitted) does not reproduce the wave height distribution nearly as well because the nearshore bathymetry was not based on nautical charts. One of the most significant but subtle differences from previous models based on the reverse fault source is the peak located at the mouth of the Bliri River. This is due to the reflection and refraction of the wave over and around the upraised block. This runup characteristic cannot be reproduced by any other tsunami source because it depends on both the source wavelength and the source location. As other researchers have found by trial and error, it turns out that a 7 km wavelength located above the eastern half of the amphitheatre does the job (Piatanesi and Heinrich, submitted). Simulated tsunami features are consistent with the scaling analyses of Watts (1998, 2000).

All numerical simulations based on the Kairei bathymetry and employing a tsunami source near the amphitheatre, including our own, produce tsunami arrival first at Malol due to faster wave propagation along the submerged canyon. Malol is located next to the head of the canyon. If slump failure does indeed correspond to the 4.4 aftershock noted by the USGS, then the tsunami arrives at Malol one or two minutes after the coupled aftershocks, which agrees with eyewitness accounts. Arrival time at Aitape also agrees with eyewitness accounts (Davies, 1998a). Moreover, the simulated tsunami converges from both sides with a horseshoe shape onto the villages of Arop as recounted by survivors (Davies, 1998a). However, this wave arrived several minutes after the aftershocks, which survivors from the Spit did not recall. This apparent discrepancy might be explained by the abundance of evidence of

liquefaction on the sand Spit (Davies, 1998a; Kawata et al., 1999). A liquefied layer of sediment is known to filter out ground motions, thereby reducing the likelihood of feeling strong aftershocks. This discrepancy still needs further investigation, however a single slump with the location, size, and displacement observed is able to explain most of the local tsunami features.

7. Conclusions

Offshore surveying including multibeam bathymetry, sub-bottom profiling, sediment coring, visual observation and rock sampling, supported by new modeling demonstrates that the most probable source of the local tsunami of July 17th 1998 that struck the Sissano area was a sediment slump located just offshore of the Lagoon in the area we term the amphitheatre. This conclusion is in accord with much of the previously acquired evidence from survivors, onland investigation and seismology. We propose the slump to be formed in cohesive sediments that failed by rotational faulting. The slump location is in the eastern part of the amphitheatre feature that lies below the Sissano Lagoon.

No major seabed trace of the thrust fault of the earthquake rupture was observed. Faults are located at the foot of the amphitheatre, bounding the southern and northern sides of the upraised block but these are either normal (40-Kilometre Fault) or with a vertical overthrust component of cm (14-Kilometre Fault), in neither case satisfying the earthquake rupture mechanism. No evidence of a blind thrust was found.

Offshore surveying immediately after a tsunami, in the context of other studies (as described) provides essential data for comparing alternative tsunami source mechanisms, such as fault and slump as well as discriminating between them. It also allows the geological framework in which tsunami generation takes place to be defined.

The Sissano area is particularly vulnerable to tsunami strike because of its location at the boundary (almost a triple junction) between the Australia, Caroline and North Bismarck Sea plates. In this region the new swathe bathymetry shows offshore northern PNG to be structurally complex and to comprise an active convergent margin system subject to subduction erosion along the inner wall of the New Guinea Trench. The convergence is transpressional. Along-strike variation in morphology is interpreted to reflect the presence of different structural units, the diachronous juxtaposition of which results in a variation in faulting type: mainly strike-slip in the east and dip-slip in the west. The area offshore of Sissano is located at the transition zone of the structural units and as a result is undergoing active subsidence and collapse. The subsidence is mainly by dip-slip faulting in rock as well as faulting and slumping in cohesive sediments. The westward advance of the collision zone between the Australia and North Bismarck Sea plates results in an increased rate of deformation. The deformation observed provides a structural context to the tsunami generating mechanisms operating in the area.

The local sedimentary regime combined with the tectonic framework of the area provides a

dominant control on sediment failure and thus to tsunami generation. The area offshore north PNG is sediment starved with mainly clay deposition. Outside of depressions and basins, sediment on steep slopes is fine grained, cohesive and stiff. The combination of stiff clays and steep slopes increases the likelihood of mass failure. Geographical variation in sediment thickness and the distribution of prospective control faults determine the location of failure.

Cold water venting around the margins of the amphitheatre supports chemosynthetic communities, and is interpreted as evidence of active faulting and fissuring as well as sediment compaction. Variations in the concentrations of faunas together with variation in the location of active venting and sulphide rich sediments allows discrimination between active and less active seabed deformation in the form of faults and slumps. Variations in extant mussel shell size may enable the timing of deformation to be elucidated.

Although the historical evidence for northern PNG is contradictory regarding tsunami events (Ripper et al., 1999), there is no doubt that the Sissano Lagoon area is vulnerable to tsunami attack because, in addition to the threat from offshore, the area is low-lying and is actively subsiding. Shallow dipping thrust planes may be the cause of the subsidence. These thrusts are also considered to be forming depressions offshore such as the Yalingi Canyon area. Further coseismic subsidence of the Lagoon area will increase the threat of significant flooding during any future tsunami attack.

Acknowledgements: The surveys would not have taken place without the foresight of Alf Simpson, Director of SOPAC in stimulating the research nor without JAMSTEC that provided the research vessels Kairei and Natsushima. The authors wish to express their appreciation to both organisations for their support in the study as well as to Captains Yakawa and Saito and to the Commander of the Dolphin Mr Yoda together with the NME technicians and crews for their help and assistance. They also thank JAMSTEC for financial support enabling them to participate in the PNG offshore surveys, to the Government of PNG for permission to carry out the surveys and to their shipboard colleagues for hours of stimulating and provoking discussion. The paper was greatly strengthened by reviews from Eric Geist and Doug Masson. Dave Tappin acknowledges Russell Lawley, Jim Rayner and Paul Williamson for assistance with the Figures and publishes with the permission of the British Geological Survey, Natural Environment Research Council, United Kingdom. Phil Watts acknowledges the financial support of the US National Science Foundation and US FEMA, the personal encouragement of Prof. Costas Synolakis, and the tsunami simulation codes provided by Profs. Fumi Imamura and Ahmet Yalciner. Gary McMurtry thanks Tom Gregory for able assistance with the sediment cores. The authors thank Philippe Heinrich, Eli Silver and Suzanne Sweet for prepublication access to their data and papers. This is SOEST contribution no. 0000

REFERENCES

- Botz, R., Faber, E., Whiticar, M.J. and Brooks, J.M., 1988. Authigenic carbonates in sediments from the Gulf of Mexico. *Earth Planet Sci. Lett.* 88. 263-272.
- Campbell, K.A. and Bottjer, D.J., 1993. Fossil cold seeps. *Nat. Geog. Res. and Expl.* 9. 326-343.
- Davies, H.L., 1990. Structure and Evolution of the Border region of New Guinea. In: Carmen, G.J. and Z., (Editors), *Petroleum Exploration in Papua New Guinea; Proceedings of the First PNG Petroleum Conference, Port Moresby, 12th-14th Feb 1990.* Pp. 245-269.
- Davies, H.L., 1998a. *The Sissano Tsunami 1998.* University of Papua New Guinea Printery, Port Moresby.
- Davies, H.L., 1998b. Geology of the Aitape Coast: Transpressional faulting and uplift in the forearc of the New Guinea Trench (abs.), *Eos Trans. Am. Geophys. Union.* 79, Fall Meeting. Suppl. F563-4,
- DeMets, C., Gordon, R.G., Argus, D.F. and Stein, S., 1994. Effect of recent revisions to the geomagnetic reversal time scale. *Geophysical Res. Lett.* 21. 2191-2194.
- Geist, E. L., 1998b. Source characteristics of the July 17, 1998 Papua New Guinea Tsunami, (abs.), *Eos Trans. Am. Geophys. Union.* 79, Fall Meeting. Suppl. F571-2.
- Geist, E.L., 2000, Origin of the 17 July 1998 Papua New Guinea Tsunami: Earthquake or Landslide. *Seis. Res. Lett.* 71. 344-351.
- Goldsmith, P., Barnett, A., Goff, J., McSaveny, M., Elliot, S. and Nongkas, M., 1999. Report of the New Zealand reconnaissance team to the area of the 17 July tsunami at Sissano Lagoon, Papua New Guinea. *Bull. N. Z. Soc. Earthquake Eng.* 32. 102-118.
- Grilli, S. T., and Watts, P. (1999). Modeling of waves generated by a moving submerged body: Applications to underwater landslides." *Engrg. Analysis with Boundary Elements*, 23(8), 645-656.
- Hecker, B., 1985. Fauna from a cold-sulfur-seep in the Gulf of Mexico: Comparison with hydrothermal vent communities and evolutionary implications. *Bull. Bio. Soc. Wash.* 6. 465-473.
- Hegarty, K.A. and Weissel, J.K. 1988. Complexities in the development of the Caroline Plate region: western equatorial Pacific. In: Nairn, A. E. M., Stehli, F.G. and Uyeda, S. (Editos) *The Ocean Basins and Margins 7B The Pacific Ocean.* Plenum Press, New York and London. pp. 277-301

Herzer, R.H., & Exon, N.F., 1985. Structure and basin analysis of the southern Tonga forearc. In: Scholl, D.W., & Vallier, T.L. (Editors.) *Geology and offshore resources of Pacific island arcs-Tonga region*. Circum-Pacific Council for Energy and Resources, Earth Science Series. 2. pp. 55-74.

Hovland, M. Talbot, M.R., Qvale, H., Olaussen, S. and Aasberg, L., 1987. Methane related carbonate sediments in pockmarks of the North Sea. *J. Sediment. Pet.* 57. 881-892.

Hurakawa, N., 1998. A fault plane of the 1998 Papua New Guinea earthquake estimated from relocated aftershocks using data of the International Data Center of CTBT. *Zisin.* 52. 95-99 (in Japanese).

Imamura, F., and Goto, C. 1988. Truncation error in numerical tsunami simulation by the finite difference method. *Coastal Engrg. in Japan*, 31(2), 245-263.

Johnson, T. and Molnar, P., 1972. Focal mechanisms and plate tectonics of the southwest Pacific. *J. Geophys. Res. B.* 77(26). 5000-5032.

Jorgensen, N.O., 1992. Methane derived carbonate cementation of marine sediments from the Kattegat, Denmark: geochemical and geological evidence. *Mar. Geol.* 103. 1-13.

Kanamori, H. and Kikuchi, M., 1993. The 1992 Nicaragua earthquake: a slow tsunami earthquake associated with subducted sediments. *Nat. A.* 361. 714-716.

Kawata, Y., Benson, B. C., Borrero, J. L., Davies, H. L., de Lange, W. P., Imamura, F., Letz, H., Nott, J. and Synolakis C., 1999. Tsunami in Papua New Guinea was as intense as first thought. *Eos, Trans. Am. Geophys. Union.* 80(9). 101,104-105

Kikuchi, M., Yamanaka, Y., Abe, K. and Morita, Y., 1999. Source, rupture process of the Papua New Guinea earthquake of July 17th 1998 inferred from teleseismic body waves. *Earth Planets Space.* 51. 1319-1324.

Kulm, I.D. and Suess, E., 1990. Relationship of carbonate deposits and fluid venting: Oregon accretionary prism. *J. Geophys. Res. B.* 95. 8899-8916.

Matsumoto, R., 1990. Vuggy carbonate crusts formed by hydrocarbon seepage on the continental shelf of Baffin Island, northeast Canada. *Geochem. J.* 24. 143-158.

Moore, J.C., Carson, B., Lewis, B.T., Ritger, S.D., Kadko, D.C., Thornburg, T.M., Embley, R.W., Rugh, W.D., Massoth, G.J., Langseth, M.R., Cochrane G.R. and Scamman, R., 1986. Oregon subduction zone: Venting, fauna and carbonates, *Science.* 231. 561-566.

Le Pichon, X., Iiyama, T., Boulegue, J., Charvet, J., Faure, M., Kano, K., Lallemand, S., Okada, H., Rangin, C., Taira, A., Urabe, T. and Uyeda, S., 1987. Nankei Trough and Zenusu Ridge: A deep submersible survey. *Earth Planet Sci. Lett.* 83. 285-299.

- Lutz, R. A., Fritz, L. W. and Rhoads, D. C., 1985. Molluscan growth at deep-sea hydrothermal vents, *Bull. Biol. Soc. Wash.* 6. 199-210.
- Matsuyama, M., Watts, P. and Yeh, H. 1999. Numerical simulation of the July 1998 Papua New Guinea tsunami using the new bathymetry from SOS1. KR98-13 cruise report-Papua New Guinea. 86-105.
- Matsuyama, M., Walsh, J.P. and Yeh, H. 1999. The effect of bathymetry on tsunami characteristics at Sissano Lagoon, Papua New Guinea. *Geophys. Res. Lett.* 26. 3513-3516.
- McCue, K. F., 1998. An AGSO perspective of PNG's tsunamagenic earthquake of 17 July 1998. *AusGeo Int.* 9.
- McSaveny, M.J., Goff, J.R., Darby, D.J., Goldsmith, P., Barnett, A., Elliot, S. and Nongkas, M., 2000. The 17 July 1998 tsunami, Papua New Guinea: evidence and initial interpretation. *Mar. Geol.* 170. 81-92.
- Milsom, J., Masson, D. and Nichols. G., 1992a. Three trench endings in eastern Indonesia. *Mar. Geol.* 104. 227-241.
- Milsom, J., Masson, D., Nichols. G., Sikumbang, N., Dwiyanto, B., Parson, L. and Kallagher, H., 1992b. The Manokwari Trough and the western end of the New Guinea Trench. *Tectonics*, 11. 145-153.
- Neuhauss, R., 1911. *Deutsch Neu-Guinea. Band 1, 22-27.* Verlag Dietrich Reimer (Ernst Vohson) Berlin.
- Neumann, A.C., Paull, C.K., Commeau, J., Chanton, J., Martens, C., Gardemal, M., Trumbull, W. and Showers, W., 1988. Abyssal seep cementation: West Florida escarpment. *Bull. Amer. Ass. Pet. Geol.* 72. 228.
- Newman, A. V. and Okal, E. A., 1998b. Moderately Slow Character of the July 17, 1998 Sandaun Earthquake as Studied by teleseismic Energy Estimates, (abs.), *Eos Trans. Am. Geophys. Union.* 79, Fall Meeting. Suppl. F564.
- Nix, E. R., Fisher, C. R., Vodenichar, J. and Scott, K. M., 1995. Physiological ecology of a mussel with methanotrophic endosymbionts at three hydrocarbon seep sites in the Gulf of Mexico. *Mar. Bio.* 122. 605-617.
- Norvick, M. and Hutchison, D.S., 1980. Aitape-Vanimo, Papua New Guinea. 1:250,000 Geological Series – Explanatory Notes. Department of Minerals and Energy. Geological Survey of Papua New Guinea.
- Orange, D.L., Greene, G.H., Reed, D., Martin, J.B., Ryan, W.B.F., Maher, N., Stakes, D. and

- Barry, J., 1999. Widespread fluid expulsion on a translational continental margin: Mud volcanoes, fault zones, headless canyons, and organic-rich substrate in Monterey Bay, California. *Bull. Geol. Soc. Am.* 111. 992-1009.
- Paull, C.K., Hecker, R., Freeman-Lynde, R.P., Neumann, C., Corso, W.P., Golubic, S., Hook, J.E., Siks, E. and Curray, J., 1984. Biological communities of the Florida escarpment resemble hydrothermal vent taxa. *Science*. 226. 965-967.
- Paull, C.K., and Neumann, A.C., 1987. Continental margin brine seeps: Their geological consequences. *Geology*. 15. 545-548.
- Paull, C.K., Chanton, J.P., Coston, J.A. and Martens, C.S., 1992. Indicators of methane derived carbonate and chemosynthetic organic carbon deposits: examples from the Florida escarpment. *Palaios*. 7. 361-375.
- Piatanesi, A. and Heinrich, P., submitted . Source characteristics of the July 17, 1998 Papua New Guinea tsunami inferred from run-up data. *J. Geophys. Res. B*.
- Ripper, I.D., 1975. Some earthquake focal mechanisms in the New Guinea/Solomon Islands region, 1963-68. Bureau Minerals Resources Australia. Report 178. (NG8).
- Ripper, I.D and Letz, H., 1999. The Sissano Lagoon (Aitape) Tsunami: which earthquake was responsible? Papua New Guinea Geological Survey Report. 99/7.
- Ritger, S., Carson, B. and Suess, E., 1987. Methane derived authigenic carbonates formed by subduction induced pore water expulsion along the Oregon/Washington margin. *Bull. Geol. Soc. Am.* 98. 147-156.
- Roberts, H.H. and Whelan, T., 1975. Methane-derived carbonate cements in barrier and beachsands of a sub-tropical delta complex. *Geochem. Cos. A*. 39. 1085-1089.
- Satake, K. and Tanioka, Y., 1999. The July 1998 Papua New Guinea Earthquake and Tsunami: A generation model consistent with various observations. (abs.), *Eos Trans. Am. Geophys. Union*. 80, Fall Meeting. Suppl. F750.
- Schwab, W. C., Lee, H. J., Twichell, D. C., 1993. Submarine landslides: Selected studies in the U.S. Exclusive Economic Zone. *Bull. U. S. Geol. Sur.* 2002, U.S., Dept. of Interior, Washington, D.C.
- Seno, T. and Kaplan, D.E., 1988. Seismotectonics of Western Papua New Guinea. *J. Phys. Ear.* 36. 107-124.
- Sibson, R.H., 1981a. Fluid flow accompanying faulting: Field evidence and models. In: Simpson, D.W. and Richards, P.G. (Editors). *Earthquake prediction: An international review*. American Geophysical Union Maurice Ewing Series. No. 4. pp. 593-603.

- Sibson, R.H., 1981b. Controls on low stress hydro-fracture dilatancy in thrust wrench and normal fault terranes. *Nature*. A. 289. 665-667.
- Smith, E. B., Williams, F. M. and Fisher, C. R., 1997. Effects of intrapopulation variability on von Bertalanffy growth parameter estimates from equal mark-recapture intervals. *Can. J. Fish. Aquat. Sci.* 54. 2025-2032.
- Smith, E. B., Scott, K. M., Nix, E. R., Korte, C., and Fisher, C. R., 2000. Growth and condition of seep mussels (*Bathymodiolus childressi*) at a Gulf of Mexico brine pool. *Ecology*. 81. 2392-2403.
- Stevens, C., McCaffrey, R., Silver, E.A., Sombo, Z., English, P. and van der Kevie, J., 1998. Mid-crustal detachment and ramp faulting in the Markham Valley, Papua New Guinea. *Geology*. 26. 847-850.
- Suess E., Carson, B., Ritger, S., Moore, J.C., Jones, M., Kuhn, I.D. and Cochrane, G., 1985. Biological communities at vent sites along the subduction zones of Oregon. *Bull. Bio. Soc. Wash.* 6. 475-484.
- Sweet, S. and Silver, E.A., . in press. Seismic reflection images of the source region of the 1998 Papua New Guinea tsunami. In: Watts, P., Synolakis, C. E. and Bardet, J-P. Prediction of Underwater Slide and Slump Hazards. Balkema, Rotterdam, Netherlands.
- Synolakis, C. E., Bardet, J.-P., Borrero, J. C., Davies, H. L., Grilli, S. T., Okal, E. A., Silver, E. A., Sweet, S., Tappin, D. R., and Watts, P. (submitted). Teleseismic Evidence Supports Slump Origin of the 1998 Papua New Guinea Tsunami. *Proc. Roy. Soc. Lond. A*.
- Tadepalli, S., and Synolakis, C. E., 1994. The run-up of N-waves on sloping beaches. *Proc. Roy. Soc. Lond. A*. 445. 99-112.
- Tadepalli, S., and Synolakis, C. E., 1996. Model for the leading waves of tsunamis. *Phy. Rev. Lett.* 77. 2141-2144.
- Takahashi, T. and Kawata, Y., Energy Concentration and Recurrence of the 1998 Papua New Guinea Tsunami. 1998. (abs.), *Eos Trans. Am. Geophys. Union*. 79. Fall Meeting. Suppl. F572.
- Tanioka, Y., 1999. Analysis of the far-field tsunami generated by the 1998 PNG earthquake. *Geophys. Res. Lett.* 22. 3393-3396.
- Tappin, D.R., 1994. The Tonga frontal arc basin. In: Ballance, P.F., (Editor) *South Pacific Sedimentary Basins. Sedimentary Basins of the World 2*. Elsevier. pp. 157-176
- Tappin, D.R., Matsumoto, T. and shipboard scientists. 1999. Offshore Surveys Identify

Sediment Slump as Likely Cause of Devastating Papua New Guinea Tsunami 1998. *Eos Trans. Am. Geophys. Union*, 80(30). 329, 334, 340.

Titov, V. and Gonzalez, F., 1998. Numerical study of the source of the July 1998 PNG earthquake (abs.), *Eos Trans. Am. Geophys. Union*. 79. Fall Meeting. Suppl. F564,

Tregoning, P., Lambeck, K., Stolz, A., Morgan, P., McCluskey, S.C., Van der Beek, P., McQueen, H., Jackson, R.R., Little, R.P., Laing, A. and Murphy, B., Estimation of current plate motions in Papua New Guinea from Global Positioning System observations. *J. Geophys. Res.* 103. 12181-12203.

Turekian, K. K. and J. K. Cochran, 1981. Growth rate of a vesicomid clam from the Galapagos Spreading Center. *Science*. 214. 909-911.

Turner, A. K., and Schuster, R. L., 1996. Landslides: Investigation and mitigation. Special Report 247. *Trans. Res. Board, National Academy Press, Washington, D.C*

Turner, R. D. and R. A. Lutz, Growth and distribution of mollusks at deep-sea vents and seeps, 1984. *Oceanus*. 27, 54-62.

Watts, P., 1998. Wavemaker curves for tsunamis generated by underwater landslides. *J. Waterwy Port, Coast. and Ocean Eng. ASCE*, 124(3). 127-137.

Watts, P., 2000. Tsunami features of solid block underwater landslides. *J. Waterwy Port, Coast. and Ocean Eng. ASCE*, 126(3). 144-152.

Watts, P., Grilli, S. T., and Synolakis, C. E., (submitted). Tsunami generation by submarine mass failure I: Wavemaker models. *J. Waterwy Port, Coast. and Ocean Eng. ASCE*.

Welsch, R. L., 1998. An American anthropologist in MelanAsia. A. B. Lewis and the Joseph N. Field South Pacific Expedition 1909-1913. Vol. 1: Field Diaries, 127-132. University of Hawaii Press, Honolulu.